



HAL
open science

Optical properties of GaN/AlN quantum dots

Pierre Lefebvre, B. Gayral

► **To cite this version:**

Pierre Lefebvre, B. Gayral. Optical properties of GaN/AlN quantum dots. Comptes Rendus. Physique, 2008, 9, pp.816. 10.1016/j.crhy.2008.10.008 . hal-00389996

HAL Id: hal-00389996

<https://hal.science/hal-00389996v1>

Submitted on 20 Jan 2025

HAL is a multi-disciplinary open access archive for the deposit and dissemination of scientific research documents, whether they are published or not. The documents may come from teaching and research institutions in France or abroad, or from public or private research centers.

L'archive ouverte pluridisciplinaire **HAL**, est destinée au dépôt et à la diffusion de documents scientifiques de niveau recherche, publiés ou non, émanant des établissements d'enseignement et de recherche français ou étrangers, des laboratoires publics ou privés.

Recent advances in quantum dot physics / Nouveaux développements dans la physique des boîtes quantiques

Optical properties of GaN/AlN quantum dots

Pierre Lefebvre^{a,1}, Bruno Gayral^{b,*}

^a Groupe d'étude des semiconducteurs – CNRS – Université Montpellier II, case courrier 074, 34095 Montpellier cedex 5, France

^b CEA-CNRS group “Nanophysique et Semiconducteurs”, CEA-Grenoble, INAC/SP2M, 17, rue des Martyrs, 38054 Grenoble, France

Available online 13 November 2008

Abstract

We present here a review of the peculiar optical properties of GaN/AlN quantum dots. These systems show unusually large exciton binding energies and band-offsets. Moreover, when grown along the (0001) axis in the wurtzite phase, the optical properties are dominated by huge on-axis internal electric fields, leading to a very low oscillator strength and complex dynamical behavior. It is also possible to grow GaN quantum dots in the cubic phase or along nonpolar axis of the wurtzite cell. We discuss properties of ensembles of quantum dots, as well as of single quantum dots studied by micro-photoluminescence. *To cite this article: P. Lefebvre, B. Gayral, C. R. Physique 9 (2008).*

© 2008 Académie des sciences. Published by Elsevier Masson SAS. All rights reserved.

Résumé

Propriétés optiques des boîtes quantiques GaN/AlN. Nous présentons une revue des propriétés optiques particulières des boîtes quantiques GaN/AlN. Ces systèmes sont caractérisés par une énergie de liaison excitonique et des décalages de bande exceptionnellement grands. Lorsque ces structures sont crues le long de l'axe (0001) en phase wurtzite, les propriétés optiques sont dominées par des champs électriques internes géants, qui conduisent à de très faibles forces d'oscillateur ainsi qu'à des comportements dynamiques complexes. Il est aussi possible de croître des boîtes quantiques GaN en phase cubique ou selon des axes non-polaires de la maille wurtzite. Nous discutons les propriétés d'ensembles de boîtes quantiques, ainsi que de boîtes quantiques uniques étudiées par micro-photoluminescence. *Pour citer cet article : P. Lefebvre, B. Gayral, C. R. Physique 9 (2008).*

© 2008 Académie des sciences. Published by Elsevier Masson SAS. All rights reserved.

Keywords: Quantum dot; GaN/AlN; Wurtzite phase

Mots-clés : Boîte quantique ; GaN/AlN ; Phase wurtzite

1. Introduction

Group-III nitrides such as GaN, InN, AlN and related compounds are receiving a considerable, renewed interest since the demonstration of efficient blue and ultraviolet light emitting diodes and laser diodes [1–3] based on (In,Ga)N

* Corresponding author.

E-mail addresses: lefebvre@ges.univ-montp2.fr (P. Lefebvre), bruno.gayral@cea.fr (B. Gayral).

¹ Present address: Institut de photonique et d'électronique quantiques, École polytechnique Fédérale de Lausanne, Station 3, CH-1015 Lausanne, Switzerland.

quantum wells (QWs). Such efficiency, despite high densities of nonradiative recombination centers, is commonly believed to arise from the strong localization of carriers on potential fluctuations in the disordered ternary alloy. Some authors [4–8] even assimilate these fluctuations to self-formed quantum dots (QDs), since their optical properties quite generally exhibit some typical zero-dimensional characteristics.

It is not the purpose of this article to enter the ongoing controversy on whether these QDs are real or not, or if more subtle localization mechanisms are at work [9,10]. Instead, we will review the most salient specificities of purposely grown nitride based QDs, in terms of optical properties observed by continuous-wave, time-resolved or spatially resolved spectroscopy techniques. For this article, we will specially focus on self-assembled GaN/AlN QDs, grown following the Stranski–Krastanov process, by molecular beam epitaxy [11–13] or by metalorganic vapor-phase epitaxy [14–16] on various types of substrates, namely sapphire, SiC or Si.

GaN and AlN exhibit wide band-gaps (3.4 and 6.2 eV [17–19], respectively) and consistently present strong excitonic binding energies (26 meV for GaN), because of low dielectric constants and large effective masses. The latter, together with the large band gap difference between GaN and AlN, leads to an unprecedented strength of carrier confinement. Therefore, nitride based nanostructures are, *a priori*, good candidates for the manifestation, *at higher temperatures*, of some typical QD properties observed at low T in more “mature” semiconductors, such as those discussed in the other articles of this special issue.

Nevertheless, other important characteristics of group-III nitrides play a decisive role (in addition to material quality issues that we will not discuss in detail because this quality is steadily improving). A complex valence band structure, strong coupling of electronic excitations to polar lattice vibrations and, above all, internal polarization effects drastically affect the optical properties of GaN/AlN QDs, individually or in assembly.

Indeed, quite generally, group-III nitrides exhibit a stable wurtzite crystal structure and, in most epitaxial processes, they tend to grow along the [0001], so-called c-axis. This symmetry allows for the appearance of spontaneous polarization, along this axis, as well as piezoelectric polarization, whenever the crystal undergoes a biaxial deformation in the (0001) plane. Now, despite their III–V nature, these compounds exhibit extremely strong polarization coefficients, as theoretically predicted [20,21] and rapidly confirmed by experiments [22–27]. Therefore, in heterostructures grown along the c-axis, electric fields of several MV/cm are present. It is the difference of *total* polarization between the QW (or QD) materials and the barrier that induces fixed charge accumulation at interfaces, leading to those huge fields. Contrary to CdTe– [28] or InAs-based [29] zinc-blende quantum structures grown along the [111] axis, where only piezoelectric fields are allowed, the interplay between spontaneous and piezoelectric contributions depends on the chemical composition of the different materials: dominated by piezoelectric effect in $\text{In}_x\text{Ga}_{1-x}\text{N}/\text{GaN}$ systems, the field is caused by both effects in a balanced way for GaN/ $\text{Al}_x\text{Ga}_{1-x}\text{N}$ associations [20,21]. The use of quaternary alloys even permits to cancel the field completely [30,31] by exact compensation of the two effects.

GaN/AlN QWs and QDs exhibit the largest electric fields estimated so far with reported experimental values ranging between 5.5 and 9.0 MV/cm [12,32–35]. In the following, we will refer to these systems as “polar QDs”.

Although more tedious, the growth of cubic GaN/AlN QDs along the [001] axis permits to observe field-free QDs [33]. It is also possible to grow wurtzite QDs along the nonpolar [11–20] axis, which drastically reduces – if not cancels – the internal field. We will therefore call “nonpolar” both latter types of QDs.

This article is organized as follows: The next paragraph is devoted to polar QDs, emphasizing: (1) specific difficulties for interpreting macroscopic continuous or time-resolved (TR-) photoluminescence (PL), (2) 1.55 μm intra-band optics favored by the broken mirror-symmetry, (3) individual properties of isolated QDs. Comparable issues are discussed for nonpolar QDs in a third paragraph, followed by concluding remarks.

2. Polar GaN/AlN quantum dots

Although the microscopic description of fields, energies and envelope functions of electrons and holes in realistic GaN/AlN QDs is complicated [36,37], it is well understood that the energies and lifetimes of excitonic recombinations are mainly driven by the dominant quantum-confined Stark effect (QCSE), which we could as well call “quantum-confined Franz–Keldysh effect”. Indeed the magnitude of the electric field would be strong enough to ionize excitons if the separated electron and hole were not contained by high potential barriers, as illustrated by Fig. 1(a) with the case of a 14 ML-wide QW (1 ML = 0.26 nm). Indeed, it has been proved [37] that an effective-QW modeling of optical transitions provided nearly identical results as a complete 3-dimensional description.

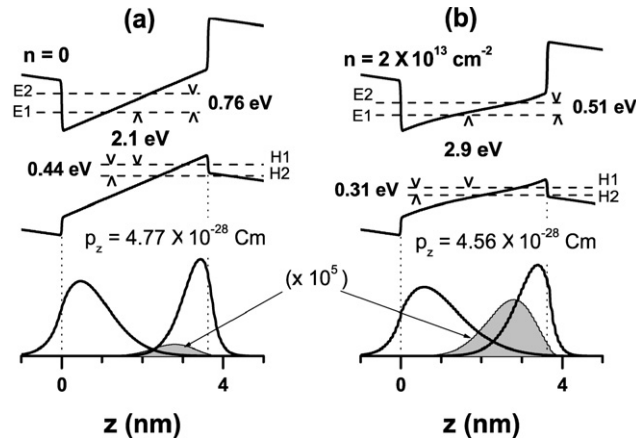


Fig. 1. (a) Shows the calculated properties of a 14 ML-wide GaN/AlN QW under weak excitation, i.e. with no electron-hole pairs present ($n = 0$). (b) Shows the result of a self-consistent solution of Schrödinger and Poisson equations for $n = 2 \times 10^{13} \text{ cm}^{-2}$. The first two electron (E1 and E2) and hole (H1 and H2) levels are displayed, with mention of the various relevant inter-subband energies. The envelope functions for the E1 and H1 states are represented in the lower part of the figure, together with their product, shown by gray areas. The values of the e–h dipole moment p_z in these two extreme situations are displayed, too.

Fig. 1. (a) Modélisation de la structure électronique d'un puits GaN/AlN de 14 monocouches sous faible excitation, c.à.d. en l'absence de porteurs ($n = 0$). (b) Résultat d'un calcul Poisson–Schrödinger auto-consistant pour $n = 2 \times 10^{13} \text{ cm}^{-2}$. Les deux premiers niveaux d'électrons (E1 et E2) et de trous (H1 et H2) sont représentés, avec les énergies inter-sous-bandes correspondantes. Les fonctions enveloppes pour les états E1 et H1 sont représentés en bas de la figure, avec leur recouvrement (en grisé). Les valeurs des moments dipolaires électron-trou p_z correspondants dans ces deux situations extrêmes sont également indiquées.

2.1. Collective emission spectra

Internal fields are so large that most transition lines are observed at energies well below the band gap of strained GaN, because the QCSE widely dominates over confinement for QD heights larger than ~ 2 nm, typically [12,32,33,38–40]. Lateral confinement effects are negligible, in comparison, due to a large aspect ratio and large effective masses. Moreover, usual size-dispersion induced broadening results more from the statistical distribution of on-axis confinement and QCSE than from lateral size fluctuation, as demonstrated recently by observation of fractionized broadening [41], where the influences of on-axis and in-plane size fluctuations are clearly separated.

Due to the electric field, QD height variation of one atomic monolayer (0.26 nm in GaN), yields energy variation over several hundred meV and therefore collective PL spectra of GaN/AlN QDs intrinsically show half-widths of comparable amounts, much larger than those reported for other materials. It has been discovered, however, that for multiple planes of polar QDs [39], the linewidth can be enhanced by another phenomenon, of primary importance in these systems: the screening of internal field by accumulation of large densities of electron-hole (e–h) pairs in the dots.

This screening is a well known property in QWs with internal fields [29], but it takes unusual magnitudes in GaN/AlN QDs, because the redshift induced by QCSE can easily reach 1 eV or even more. The important corollary to this redshift is the dramatic increase of radiative lifetimes, nearly exponential with QD height, resulting from the on-axis e–h separation, shown in Fig. 1(a). The huge radiative lifetimes make it quite easy to accumulate huge densities of pairs by using moderate optical excitation. Fig. 1(b) shows the calculated changes induced by accumulation of $2 \times 10^{13} \text{ cm}^{-2}$ e–h pairs. The fundamental transition is blue-shifted by 0.8 eV and the e–h wave-function overlap is increased over orders of magnitude. The CNRS team in Montpellier (GES-University of Montpellier) performed systematic, detailed studies of these issues, in collaboration with the CRHEA-CNRS in Valbonne. These studies [35,38,39] revealed that it was practically impossible, in continuous-wave (cw) PL experiments, to avoid the blueshift of optical transitions, with differential effects on the different dot sizes and on the different QD planes, in case of stackings of them.

In practice, measuring values as simple as the “true” PL recombination energy and lifetime requires drastic experimental care, as exemplified in Fig. 2: the time-dependent PL spectrum of a stacking of polar QDs shifts by more than 0.8 eV as time goes from a few ns to a few tens of μs , keeping a constant FWHM of ~ 250 meV and decreasing

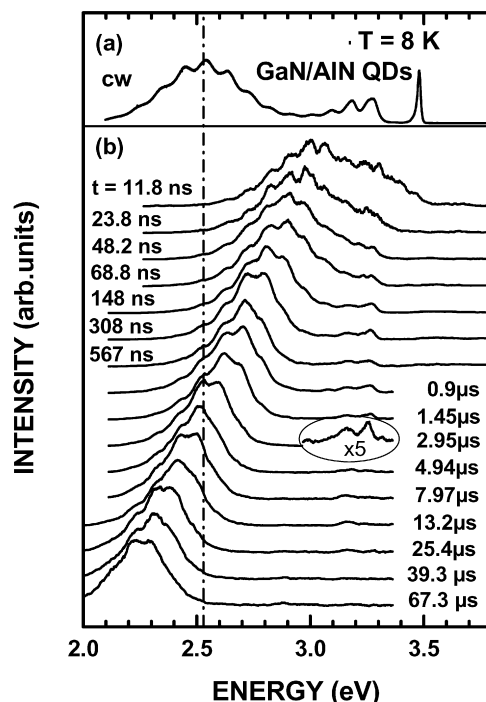


Fig. 2. In (a), the cw PL spectrum of a sample with 10 planes of GaN/AlN QDs having typical heights of 4.3 nm. (b) The PL spectra recorded at different delays after the pulsed laser excitation. For clarity, the spectra have been normalized in intensity. The position of the peak of cw PL is shown by the dash-dotted line. For short delays, the spectrum is artificially broadened by the presence of the long-lived PL at 3.2 eV, arising from defects in the GaN buffer layer, whose short-lived PL line appears at 3.48 eV.

Fig. 2. (a) Spectre de PL sous excitation continue d'un échantillon avec 10 plans de boîtes quantiques GaN/AlN de hauteur typique 4,3 nm. (b) Spectres de PL après différents délais sous excitation impulsionnelle. Les spectres sont normalisés en intensité. La position du pic de PL obtenu en (a) est indiquée par la ligne trait-point. Aux temps courts, le spectre est élargi artificiellement par la présence de luminescence à 3,2 eV provenant de défauts dans la couche tampon de GaN.

intensity over four orders of magnitude. This results from the progressive “de-screening” of the field by which the radiative lifetime passes from a few ns to a few hundred μ s. For a comparison, the continuous-wave PL spectrum in Fig. 2(a) obtained in supposedly “reasonable” excitation conditions exhibits completely different – and irrelevant – peak position and linewidth. When appropriate precautions are taken, it is however possible to let the system reach a regime where the PL energy remains idle and the intensity decay is exponential with time. And, then only, one can draw a chart of experimental PL decay times versus PL energy, compatible with an effective internal field of ~ 9 MV/cm [35], as illustrated in Fig. 3.

It is crucial to remark, here, that dynamical properties such as those shown in Fig. 2, have been observed nearly identical at room temperature (RT) [39], meaning that nonradiative recombination processes are not dominant at 300 K, despite radiative lifetimes that can reach hundreds of microseconds. This demonstrates the efficiency of carrier confinement in these systems, which induces a unique robustness of interesting properties in regard of the escape of carriers that is well-documented in other material systems.

In spite of this, the “screening issues”, salient for QD heights larger than ~ 2 nm, are not favorable for injection-independent light-emitting devices, and large radiative lifetimes are not favorable for studies of single QDs such as those detailed below. Nevertheless, the extreme sensitivity of such systems to moderate optical excitations induces nonlinear optical properties at unprecedentedly low power densities that could be useful and are still to be explored [42]. As an alternative application of the presence of such huge fields, strongly coupled dipoles in two vertically stacked GaN/AlN QDs have been theoretically investigated as building blocks for new concepts for quantum computing [43]. Concerning fundamental investigations, a detailed study of the coupling of electronic excitations with polar lattice vibrations is still lacking for polar GaN/AlN QDs. Previous studies on wide (Ga,In)N/GaN QWs and QDs proved that the large e–h dipole induces a giant coupling with optical phonons that increases with the on-axis size

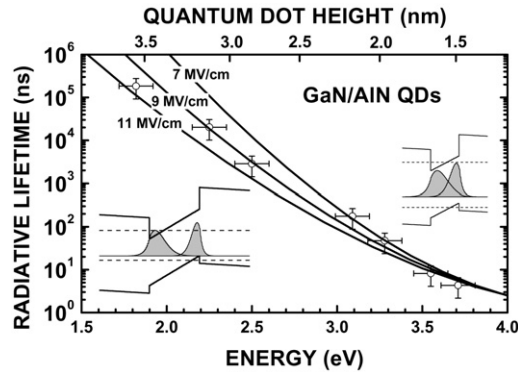


Fig. 3. Measured radiative lifetime (circles) versus measured PL energies at large time delays, for different QD samples. Solid lines show the calculated value of lifetime as a function of energy of the fundamental transition for an effective electric field of respectively 7, 9 and 11 MV/cm. Reprinted with permission from Ref. [35]. Copyright (2006) by the American Physical Society.

Fig. 3. Temps de déclin radiatif mesuré (cercles) fonction de l'énergie de luminescence mesurée aux temps longs pour différents échantillons de boîtes quantiques. Les traits pleins montrent les valeurs calculées de temps de déclin en fonction de l'énergie de la transition fondamentale pour des champs électriques effectifs de 7, 9 et 11 MV/cm. Réimprimé avec permission de la référence [35]. Copyright (2006) American Physical Society.

of the system. This results in abnormally strong phonon replicas [44] that have not yet been observed, so far, for GaN/AlN QDs.

2.2. Intraband properties – unipolar optical devices

Another interesting possibility to consider is the use of intraband transitions in III-N heterostructures. In this respect GaN/(Al,Ga)N heterostructures show some interesting peculiarities. First of all, the huge conduction band-offset between GaN and AlN around 1.7 eV [45] allows one to tune electron intraband transitions to 0.8 eV, i.e. around 1.55 μm which is the choice wavelength for long-haul telecom applications. The second reason is that due to the large electron effective mass (0.2) and the large LO-phonon energy (90 meV), the LO-phonon scattering is very efficient and leads to very fast recovery times of these transitions (150 to 400 fs). Thus GaN/(Al,Ga)N heterostructures offer interesting prospects for ultra-fast telecom wavelengths intraband detectors. One has to note that due to the large electron effective mass in GaN, very thin layers (down to ~ 1 nm) have to be grown in order to reach the telecom wavelength range. Of course the QCSE has to be taken into account to calculate the transition energies and oscillator strengths of the intraband transitions, and it notably makes the transitions between same-parity states allowed.

Gmachl et al. were the first to demonstrate near-infrared intraband absorption in GaN/(Al,Ga)N quantum wells [46], while Moumanis et al. demonstrated the same effect on QDs [47]. It has to be noted that due to the weak lateral confinement in GaN QDs, the polarization selection rules for intraband transitions are the same for QDs and QWs in the telecom wavelength range, namely an absorption is obtained only for TM-polarized guided waves. Research is on-going on this topic, with notable progresses both in growth and processing of the intraband devices, with for instance the recent demonstration of a QD-based intraband photodetector up to room temperature [48,49] as shown in Fig. 4. Let us note that potential advantages of QDs over QWs for this application, such as lower dark current, have not been demonstrated yet, as in both cases the dark current is pinned by the high dislocation density.

2.3. Single dot spectroscopy

Following the trend of other material systems, experimental developments have been performed in several groups in order to adapt micro-PL setups to ultraviolet-visible ranges of the spectrum and therefore propose spectroscopic studies of individual GaN/AlN QDs. In addition to technical difficulties related to confocality of the setups in the visible/ultraviolet, the mastering of low QD densities, of QD isolation and of low densities of radiative defects in AlN barriers have been the critical issues that had to be dealt with prior to any detailed study. Moreover, the vertical size of the QDs had to be limited, to preserve small radiative lifetimes and therefore preserve reasonable signal-to-noise ratios at the scale of single emitting QDs.

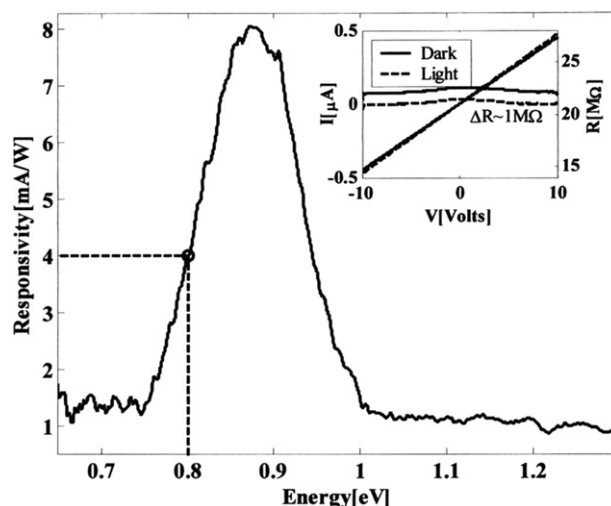


Fig. 4. Spectral responsivity of an infrared photodetector based on GaN/AlN QDs of typical height 1.1–1.3 nm. The inset displays the I–V characteristic with and without illumination. Reprinted with permission from Ref. [49]. Copyright (2006) American Institute of Physics.

Fig. 4. Réponse spectrale d'un photodétecteur infrarouge à base de boîtes quantiques GaN/AlN de hauteur typique 1,1–1,3 nm. L'encart montre la caractéristique courant-tension d'obscurité et sous illumination. Réimprimé avec permission de la référence [49]. Copyright (2006) American Institute of Physics.

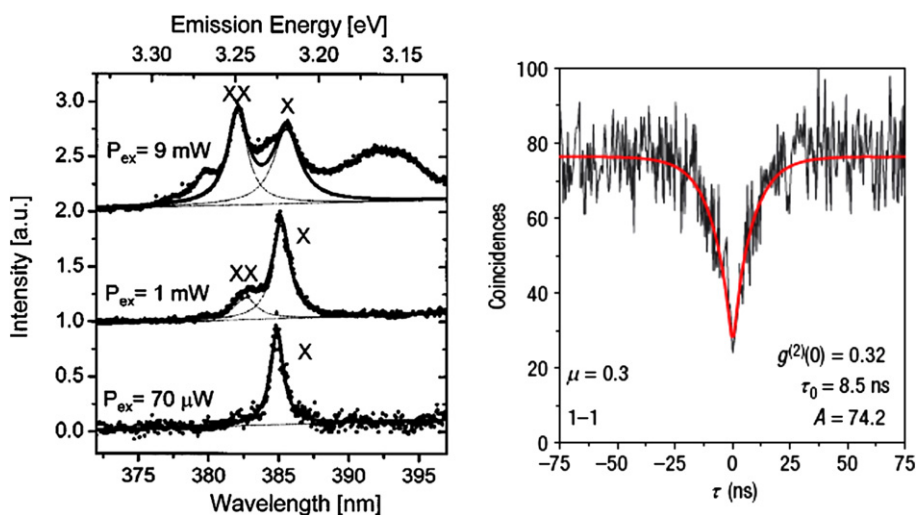


Fig. 5. (Left) Excitonic and biexcitonic PL lines from an isolated GaN/AlN QD, at 3.5 K. Reprinted from Ref. [40]. (Right) Autocorrelation measurement on a single GaN QD showing antibunching behavior. Reprinted with permission from Ref. [40]. Copyright (2004) American Institute of Physics. Reprinted with permission from Macmillan Publishers Ltd: Nature Materials (Ref. [51]), copyright (2006).

Fig. 5. (Gauche) Raies excitoniques et biexcitoniques d'une boîte quantique unique GaN/AlN à 3,5 K. Réimprimé de la Ref. [40]. (droite) Mesure d'autocorrélation sur une boîte quantique unique ; caractéristique d'un dégroupement de photons. Réimprimé avec permission de la référence [40]. Copyright (2004) American Institute of Physics. Réimprimé avec permission de Macmillan Publishers Ltd : Nature Materials (référence [51]), copyright (2006).

The first results came from Y. Arakawa's group (see Fig. 5), who reported surprisingly broad PL lines from isolated polar QDs and then detailed studies of excitonic versus bi-excitonic optical transitions [40], eventually demonstrating possible control of single photon emission by photon anti-bunching experiments, up to $T = 200$ K [50,51], and showing promising control of Stark effect [52,53].

European groups in Grenoble, Montpellier, Valbonne and Lausanne have reported further single-dot investigations on GaN/AlN QDs. It is worth mentioning here that micro-PL studies on single (In,Ga)N/GaN QDs have also been recently published (see e.g. Refs. [8,54]).

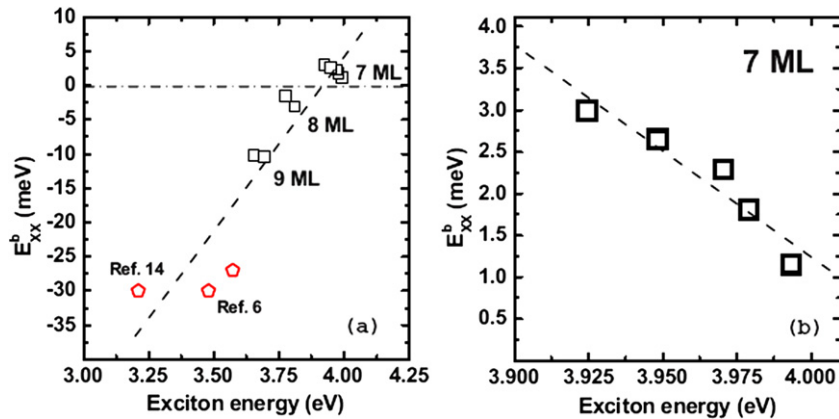


Fig. 6. (a) Dependence of the biexcitonic binding energy E_{XX}^b on the exciton emission energy for GaN/AlN QDs of different vertical sizes. (b) Dependence of E_{XX}^b on the exciton emission energy for QDs with the same vertical size (7 ML). Dashed lines are linear fits used as a guide for the eye. References 6 and 14 in the figure stand for the present Refs. [51] and [40] respectively. Reprinted with permission from Ref. [41]. Copyright (2008) by the American Physical Society.

Fig. 6. (a) Variation de l'énergie de liaison biexcitonique E_{XX}^b en fonction de l'énergie d'émission excitonique pour des boîtes quantiques de hauteurs différentes. (b) Variation de l'énergie de liaison biexcitonique E_{XX}^b en fonction de l'énergie d'émission excitonique pour des boîtes quantiques de même hauteur (7 monocouches). Les lignes pointillées sont des ajustements linéaires. Les références 6 et 14 dans la figure sont respectivement les Refs. [51] et [40] du présent article. Réimprimé avec permission de la référence [41]. Copyright (2008) American Physical Society.

One favorable point that results from internal fields is the fact that exciton and biexciton lines can have quite different emission energies, because of large biexcitonic correlation energy. A recent study [41] proved that, indeed, this correlation energy depends strongly on the vertical and lateral sizes of the QDs, as shown in Fig. 6. The binding energy can be either negative, for small QD heights where quantum confinement dominates over QCSE, but also positive when dominant field effects enhance the electron–electron and hole–hole repulsive terms, which occurs for larger dot heights. Finally, Renard et al. recently demonstrated very large biexciton binding energies – in the 20–40 meV range – for GaN quantum dots embedded in nanowires [55] emitting around 4 eV.

In addition to weak carrier escape rates, possibly large energy difference between single and double excitons is a promising argument in favor of a possible utilization of such systems for controlled single-photon emitters *operating at room temperature*. Now, the ultimate problem to investigate in this perspective is the mechanism of broadening of emission lines, especially for high temperatures.

In the most recent studies [41,56,57] PL linewidths appeared significantly smaller than in the pioneer works by Arakawa group. Although, the complete study of broadening mechanisms (e.g. versus temperature) are yet to come for polar GaN/AlN QDs, it is now clear that electrostatic effects related to charged point defects play a major role. Time-dependent single-dot emission recorded over minutes revealed that narrow emission lines (width limited by apparatus resolution) can in fact jump or slide between different energy positions [56]. This phenomenon, whose rate increases with excitation intensity, has been assigned to charging/discharging of neighboring traps. The proximity of these traps is believed to control both the magnitude and the rate of this “spectral diffusion” and therefore the large linewidths observed in the first reports were associated with larger densities of such defects. It is also believed that the strong e–h dipole induced by electric fields increases the sensitivity of excitons to electrostatic environment, especially when the QD heights are larger than ~ 3 nm, typically. This point still has to be ascertained: detailed comparison with nonpolar QDs via PL experiments with superior spectral resolution and under variable temperature are expected to provide clear answers on such issues.

Another aspect that has been investigated is the linear polarization of the light emitted by GaN/AlN single QDs. Some variable degree of polarization was found [57] on different QDs, with variable preferential axes that do not coincide with crystallographic directions. Moreover, no doublet of cross-polarized, slightly split, PL contributions was observed, contrary to what was known in CdTe–, GaAs, CdSe, or InAs-based single QDs [58–62]. The latter observation was attributed to the conjunction of some in-plane anisotropy and exchange interaction. Modeling the fine structure of GaN-based QDs emphasized a fundamental originality of these systems, namely the fact that light-hole

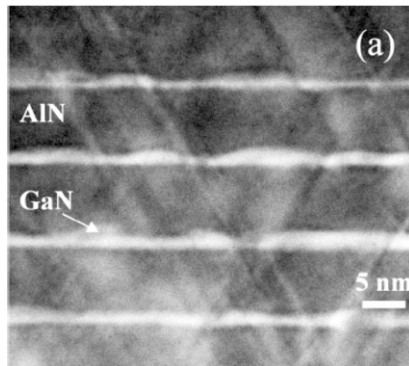


Fig. 7. Dark-field TEM image of cubic GaN/AlN QDs. The large density of stacking faults appears clearly. Reprinted with permission from Ref. [63]. Copyright (2000) American Institute of Physics.

Fig. 7. Image TEM en champ sombre de boîtes quantiques cubiques GaN/AlN. La grande densité de fautes d'empilement apparaît clairement. Réimprimé avec permission de la référence [63]. Copyright (2000) American Institute of Physics.

and heavy-hole (A and B) levels are much less split than in other systems and therefore they are mixed in a complex way. It is the ratio of the anisotropy term to this splitting that really rules the degree of polarization and, to a certain extent, the splitting of cross-polarized lines. The nonobservation of this splitting was tentatively explained, either by the charged exciton nature of the emitter or by a specific combination of long- and short-range exchange interaction terms [57].

3. Nonpolar GaN/AlN quantum dots

Due to the aforementioned complex and rich phenomena linked to the QCSE in polar wurtzite GaN QDs and the possible negative consequences in terms of device applications, it is tempting to probe the optical properties of GaN heterostructures for which the QCSE does not dominate the properties of the confined carriers, in so-called nonpolar structures. Among the nonpolar GaN/AlN QDs, one should distinguish between the cubic phase structures, and the hexagonal phase samples for which the polar *c*-axis lie along the growth plane.

3.1. Cubic phase GaN quantum dots

The first possibility to study nonpolar GaN QDs is to grow cubic phase III-N compounds that would display properties that are similar to more classical semiconductors such as arsenide or phosphide compounds, while retaining the peculiarities of a wide band-gap semiconductor. Most attempts to produce such samples were done using either GaAs substrates or 3c-SiC substrates. More specifically, GaN/AlN QDs were grown on 3c-SiC pseudo substrates on Si (001) [63], with a typical size of 1.6 nm in height and 13 nm in diameter, and a density of about 10^{11} cm^{-2} .

Such samples contain a very large density of {111} stacking faults, due to the metastable character of the *c*-AlN and *c*-GaN as shown in Fig. 7. Concerning the optical properties, Simon et al. [33] have clearly shown, by analyzing the QD height dependence of the transition energy, that there is no observable QCSE in these structures: the QDs behave basically as a regular square QW. This is even clearer when analyzing the time-resolved PL of these structures as shown in Fig. 8: in marked contrast with polar QDs, the decay time for cubic GaN QDs does not depend on the QD height and remains around 200 ps at 5 K [33].

Garayt et al. have shown that spectrally sharp lines can be obtained in cathodoluminescence on cubic GaN QDs, with linewidths in the few meV range [64]. Recently, Lagarde et al. have reported optical orientation of exciton spin up to room temperature in such cubic GaN QDs, with spin relaxation time exceeding 10 ns even at 300 K [65].

In spite of their interesting fundamental properties, there are still very few studies of cubic GaN QDs, mainly due to the difficulty to grow high quality samples.

3.2. Nonpolar wurtzite phase QDs

The other possibility to get rid of or at least reduce the internal electric field in heterostructures is to grow the wurtzite crystal along a nonpolar axis, i.e. with the *c*-axis in the plane of the layers. In that case the macroscopic

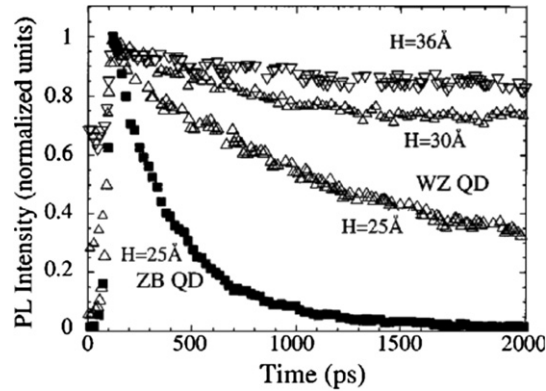


Fig. 8. PL decay curves for cubic (ZB) GaN QDs and polar hexagonal (WZ) GaN QDs of various heights at 5 K. The much higher oscillator strength of cubic QDs is here demonstrated. Reprinted with permission from Ref. [33]. Copyright (2003) by the American Physical Society.

Fig. 8. Déclin de PL à 5 K pour des boîtes quantiques GaN cubiques (ZB) et hexagonales polaires (WZ) de différentes hauteurs. La force d'oscillateur bien plus grande des boîtes quantiques cubiques est ici démontrée. Réimprimé avec permission de la référence [33]. Copyright (2003) American Physical Society.

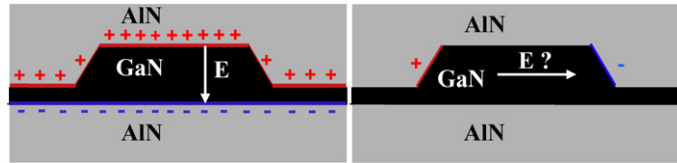


Fig. 9. Geometry difference between a polar QD and a nonpolar QD. Left: a polar QD (c-axis pointing upwards), with planar capacitor like geometry. On the right a [11–20] QD (c-axis along the plane of the page, pointing leftward) with few charges deposited on two side facets. The typical QD size is 20 nm in diameter and 2 nm in height. E denotes the internal electric field.

Fig. 9. Différence de géométrie entre des boîtes quantiques polaires et non-polaires. Gauche : une boîte quantique polaire (axe c pointant vers le haut) avec une géométrie de type condensateur planaire. A droite, une boîte quantique [11–20] (axe c dans le plan de la page, pointant vers la gauche) avec peu de charges déposées sur deux facettes latérales. La taille typique des boîtes quantiques est de 20 nm de diamètre et 2 nm de hauteur. E est le champ électrique interne.

polarization is still present as the crystal symmetry is still the same as in regular polar III-N samples. However for a QW, there is no component of the polarization perpendicular to the interfaces, so that no internal electric field builds up. This was clearly shown experimentally by Waltereit et al. [66] for m-plane GaN/AlGaIn QWs grown on a γ -LiAlO₂ (100) substrate. This first demonstration was followed by several papers on nonpolar heterostructures grown either along the [11–20] or the [1–100] axis. It should be noted that most literature on nonpolar III-N heterostructures is device-oriented, with the promise of achieving higher performance lasers and LEDs than with the polar approach for (In,Ga)N/GaN heterostructures.

Growth and optical properties of nonpolar GaN/AlN QDs were studied in the CEA-CNRS group in Grenoble, in collaboration with the University of Valencia. The situation is *a priori* much different for a nonpolar QW and for nonpolar QDs. Indeed in the case of QDs, the lateral facets do cross the polarization vectors so that an internal electric field might build up (see Fig. 9). The situation has however not much in common with that of a polar QD for which the heterostructure is embedded in a planar capacitor-type of structure.

For a nonpolar QD, the effective charge deposited on each side facet of the QD is very small (on the order of a few elementary charges), and these charged facets are well separated (QD diameter of typically 15 to 20 nm). Moreover due to the in-plane anisotropy of the grown crystal, the QD 3D-shapes and strain profiles are difficult to measure experimentally [67,68]. It is thus difficult to predict what the magnitude of the QCSE in such structures might be, as it should be very sensitive to the particular shape of the QDs, to strain gradients within the QDs and the barrier and to possible screening by residual doping. Nonetheless, Cros et al. studied this issue on a-plane QDs for a truncated pyramid with square base geometry, taking into account the strain distribution based on Raman scattering experiments and on calculations [69]. One important conclusion is that in this particular case, the piezoelectric and

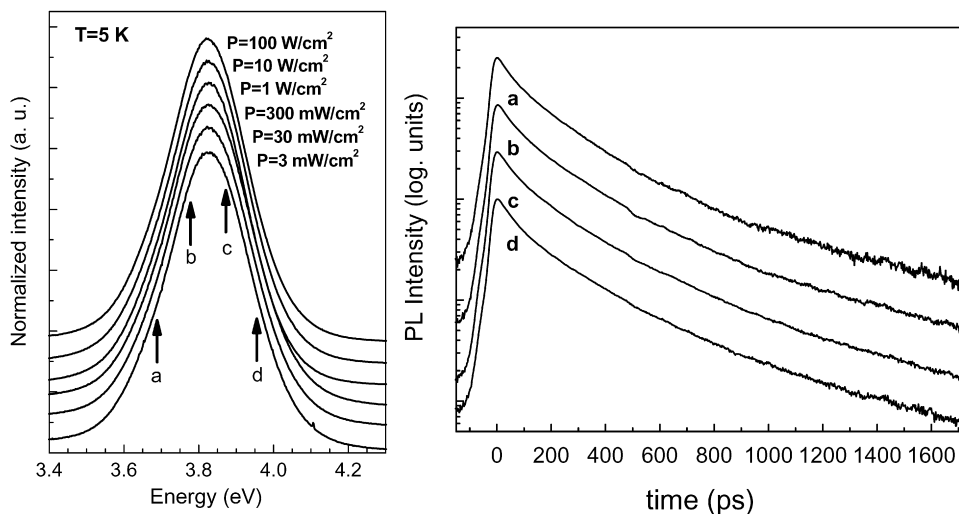


Fig. 10. cw PL spectrum as a function of excitation power density for a-plane GaN QDs (left). Corresponding time-resolved PL spectra as a function of detection energy (right). No screening is observed in cw PL, while the time-resolved data show that the decay is fast and does not depend on the QD size.

Fig. 10. Spectre de PL sous excitation continue en fonction de la densité de puissance d'excitation pour des boîtes quantiques plan a (gauche). Spectres résolus en temps correspondant en fonction de l'énergie de détection (droite). On n'observe pas d'écrantage en PL continue, et les données résolues en temps montrent que le déclin est rapide et ne dépend pas de la taille de la boîte quantique.

spontaneous components of the polarization difference are of opposite signs and thus partially cancel out. This leads to a much reduced electric field (by a factor of twelve in their calculation) compared to c-plane QDs. Moreover the electrostatic potential along the c-axis within the nonpolar QD varies smoothly across the QD, leading to weakly confining potentials. The conclusion is that the QCSE in such QDs depends strongly on the precise shape of the QD, in contrast to polar QDs for which the QCSE depends quasi-exclusively on the height of the QD as explained earlier in this article.

Experimentally, optical spectroscopy results confirm that the QCSE is much reduced for a-plane QDs compared to polar QDs of similar size. One first hint of this is given by the cw PL spectroscopy of a-plane QDs: the PL spectrum is at higher energy than the GaN bandgap for high quality QDs [70,71] (note that Fig. 3 in [70] shows weak below bandgap emission for coalesced QDs with a very high GaN coverage: in that case, it is not clear that the PL actually stems from QD luminescence and not from structural defect related luminescence).

Fig. 10 also shows that no screening effect is observed when varying the excitation power over 5 orders of magnitude in the range where QD state filling occurs, as also shown in Ref. [71]. These cw PL results already show that the optical properties are very different from what would be obtained on polar QDs of similar sizes. However, the best experiment to probe the QCSE (as already explained in Section 2.1) is to perform time-resolved PL. This is especially true in the case of nonpolar QDs for which the dimension over which the electrostatic field is applied is typically one QD diameter so that the spatial separation of the electron and hole wavefunctions can be quite large even for a weak electric field and thus even if the QCSE induced red-shift is very small. The measure of the decay time is a very fine probing of the internal electric field, particularly in this nonpolar geometry. The results displayed in Fig. 10 show that the decay time is quite short (around 250 ps) and does not depend on the emission energy (and thus does not depend on the QD size). It can then be deduced that no effect of the internal electric field can be observed in this experiment: the QCSE is too weak to be detected [72].

Nonetheless, we remark that 250 ps is not such a short decay time for emitters around 3.8 eV: it corresponds to an oscillator strength of about 10, i.e. similar to the one of InAs QDs. This shows that despite the fact that the GaN Bohr radius is 2.8 nm, i.e. much smaller than the lateral dimensions of the GaN QDs, the exciton is still laterally strongly confined in such QDs so that no giant oscillator strength phenomenon can take place. This localization phenomenon can also be probed – and was indeed confirmed – by studying the lineshape of the luminescence of a single QD as a function of temperature as shown in Fig. 11. This experiment permits to probe the coupling of excitons to acoustic phonons, from which the spatial extent of the confined wavefunctions can be estimated [72,73].

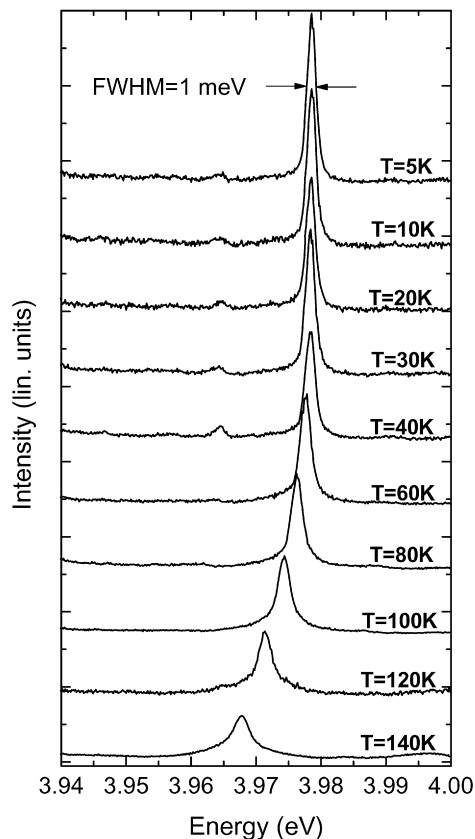


Fig. 11. Evolution of the emission lineshape of a single GaN/AlN nonpolar QD. The broadening of the line at high temperature is characteristic of coupling to acoustic phonons.

Fig. 11. Evolution de la forme de raie de PL pour une boîte quantique unique non-polaire GaN/AlN. L'élargissement à haute température est caractéristique d'un couplage à des phonons acoustiques.

Nonpolar QDs also have interesting polarization behaviors. Let us recall that in wurtzite GaN, the fundamental transition (“A-exciton”) has its dipole perpendicular to the *c*-axis. This means that in the absence of valence band mixing, the transitions observed in PL on nonpolar GaN, when observed from the top (along the growth axis) are expected to be fully polarized, perpendicularly to the *c*-axis [17]. This is confirmed for nonpolar QWs for instance [74]. Again, the situation is more complicated for QDs, as in that case due to three-dimensional confinement and strain relaxation, important band-mixing can occur, leading to a partial in-plane depolarization of the transitions [75]. For instance *a*-plane QDs show a relatively low in-plane degree of polarization (typically 60% perpendicular to the *c*-axis) [71], which depends on the QD size, while *m*-plane QDs are very strongly polarized (95% perpendicular to the *c*-axis) [76].

As a partial conclusion on nonpolar QDs, one can say that these little studied objects display rich fundamental properties that need to be further explored. Concerning possible applications, while devices based on nonpolar (In,Ga)N/GaN QWs begin to show interesting performances, the potential of nonpolar GaN/AlN QDs, notably for light emission the UV range, still needs to be assessed.

4. Conclusions

Launched less than ten years ago, a few research programs worldwide put specific interest on the prospective properties of GaN/AlN QDs, considered as building blocks for possible single photon emitters and other information processing devices operating at room temperature. Like for other physical systems, numerous steps had to be taken towards a better control of material quality and of the QD density. Existing QD isolation processes had to be adapted

to these new materials. Specific experimental setups had to be developed, in order to face new spectral and temporal ranges.

As shown in this article, despite these difficulties and the small number of groups involved, several decisive results have been obtained. Promising advances have been reported and nothing proved, to date, that the goal of RT single-photon emission is not reachable. The question of the utility of GaN QDs for efficient RT light emitting devices at short wavelengths (260 nm, typically) is still open, since a lot of technological issues have to be addressed. The same comment goes to telecom devices based on intraband transitions, where the superiority of QDs over QWs is not established.

Like for other material systems, group-III nitride QDs still necessitate more material developments and basic research to realize their high potential. Material quality issues are indeed to be addressed, specially the understanding and limitation of volume and surface defects (notably in AlN), that have detrimental consequences, via electrostatic effects, on the intensity and stability of light emission in GaN/AlN QDs. Some progress is still expected, too, in the control of the nano-objects themselves. One example of promising context for such a control of quality, size and position is the development of hybrid top-down/bottom-up growth methods and of nanocolumnar growth of defect-free III-nitride systems. Photonic aspects will also certainly receive a lot of attention in the coming years, e.g. with the development of nitride microcavities that are now reaching maturity [77]. This will improve photon extraction and give the possibility to play with exciton-photon coupling with original degrees of freedom. We also wish to remark that the interesting potential of III-nitride QDs could be extended to usual telecommunication wavelengths, not only via intraband optics: as a matter of fact InN (band-gap of 0.6 eV) receives a growing interest and shows constant progress in terms of material development. This is so far a critical point that might be solved in the coming years.

Concerning detailed physical properties, a lot has been understood concerning the role of internal fields in polar QDs and their possible utility, e.g. by enhancing the exciton-biexciton splitting. Nevertheless, a lot of knowledge is still lacking concerning, for instance, the fine structure of excitonic emission, or the detailed processes that rule line broadenings. Theoretical efforts, in particular, are especially required in order to account quantitatively for the accumulation of complexities of these systems: internal electric fields, QD shape effects, valence-band mixings, Coulomb interactions (including exchange), multi-particle states, anisotropy effects, specific hierarchy of some characteristic energies. . . .

Acknowledgements

The authors are especially indebted to all their colleagues in Montpellier, Grenoble, Valbonne, and Lausanne with whom they had the pleasure to share some of the exploration of confined structures in the III-N system over the last years.

References

- [1] S. Nakamura, T. Mukai, M. Senoh, *Appl. Phys. Lett.* 64 (1994) 1687.
- [2] S. Nakamura, G. Fasol (Eds.), *The Blue Laser Diode*, Springer, Berlin, 1997.
- [3] S. Nakamura, in: B. Gil (Ed.), *Group III Nitride Semiconductor Compounds*, Clarendon Press, Oxford, ISBN 0-19-850159-5, 1998 (Chapter 10).
- [4] D. Behr, J. Wagner, A. Ramakrishnan, H. Obloh, K.-H. Bachem, *Appl. Phys. Lett.* 73 (1998) 241.
- [5] N. Wieser, O. Ambacher, H.P. Felsl, L. Görgens, M. Stutzmann, *Appl. Phys. Lett.* 74 (1999) 3981.
- [6] K.P. O'Donnell, R.W. Martin, P.G. Middleton, S.C. Bayliss, I. Fletcher, W. Van der Stricht, P. Demeester, I. Moerman, *Mater. Sci. Eng. B* 59 (1999) 288.
- [7] K.P. O'Donnell, J.F.W. Mosselmanns, R.W. Martin, S. Pereira, M.E. White, *J. Phys.: Cond. Matter* 13 (2001) 6977.
- [8] R. Seguin, S. Rodt, A. Strittmatter, L. Reissmann, T. Bartel, A. Hoffmann, D. Bimberg, E. Hahn, D. Gerthsen, *Appl. Phys. Lett.* 84 (2004) 4023.
- [9] A. Morel, P. Lefebvre, S. Kalliakos, T. Taliercio, T. Bretagnon, B. Gil, *Phys. Rev. B* 68 (2003) 045331.
- [10] A. Hangleiter, F. Hitzel, C. Ntzel, D. Fuhrmann, U. Rossow, G. Ade, P. Hinze, *Phys. Rev. Lett.* 95 (2005) 127402.
- [11] B. Daudin, F. Widmann, G. Feuillet, Y. Samson, M. Arlery, J.L. Rouviere, *Phys. Rev. B* 56 (1997) R7069.
- [12] B. Damilano, N. Grandjean, F. Semond, J. Massies, M. Leroux, *Appl. Phys. Lett.* 75 (1999) 962.
- [13] M. Arlery, J.L. Rouvière, F. Widmann, B. Daudin, G. Feuillet, H. Mariette, *Appl. Phys. Lett.* 74 (1999) 3287.
- [14] M. Miyamura, K. Tachibana, Y. Arakawa, *Appl. Phys. Lett.* 80 (2002) 3937.
- [15] S. Kako, M. Miyamura, K. Hoshino, Y. Arakawa, *Phys. Status Solidi B* 240 (2003) 388.
- [16] K. Hoshino, S. Kako, Y. Arakawa, *Appl. Phys. Lett.* 85 (2004) 1262.

- [17] R. Dingle, D.D. Sell, S.E. Stokowski, M. Ilegems, *Phys. Rev. B* 4 (1971) 1211.
- [18] W.M. Yim, E.J. Stofko, P.J. Zanzucchi, J.I. Pankove, M. Ettenberg, S.L. Gilbert, *J. Appl. Phys.* 44 (1973) 292.
- [19] B. Monemar, *Phys. Rev. B* 10 (1974) 676.
- [20] F. Bernardini, V. Fiorentini, D. Vanderbilt, *Phys. Rev. B* 56 (1997) 10024.
- [21] F. Bernardini, V. Fiorentini, *Phys. Rev. B* 57 (1998) R9427.
- [22] A. Bykhovskiy, B.L. Gelmont, M. Shur, *J. Appl. Phys.* 81 (1997) 6332.
- [23] J.-S. Im, H. Kollmer, J. Off, A. Sohmer, F. Scholz, A. Hangleiter, *Phys. Rev. B* 57 (1998) R9435.
- [24] M. Leroux, N. Grandjean, M. Laügt, J. Massies, B. Gil, P. Lefebvre, P. Bigenwald, *Phys. Rev. B* 58 (1998) R13371.
- [25] P. Lefebvre, J. Allègre, B. Gil, H. Mathieu, P. Bigenwald, N. Grandjean, M. Leroux, J. Massies, *Phys. Rev. B* 59 (1999) 15363.
- [26] M. Leroux, N. Grandjean, J. Massies, B. Gil, P. Lefebvre, P. Bigenwald, *Phys. Rev. B* 60 (1999) 1496.
- [27] C. Wetzel, T. Takeuchi, H. Amano, I. Akasaki, *Phys. Rev. B* 61 (2000) 2159.
- [28] R. André, J. Cibert, Le Si Dang, *Phys. Rev. B* 52 (1995) 12013.
- [29] P. Boring, B. Gil, K.J. Moore, *Phys. Rev. Lett.* 71 (1993) 1875.
- [30] F. Bernardini, V. Fiorentini, *Phys. Status Solidi B* 216 (1999) 391.
- [31] P. Lefebvre, S. Anceau, P. Valvin, T. Taliercio, L. Konczewicz, T. Suski, S.P. Łepkowski, H. Teisseyre, H. Hirayama, Y. Aoyagi, *Phys. Rev. B* 66 (2002) 195330.
- [32] F. Widmann, J. Simon, N.T. Pelekanos, B. Daudin, G. Feuillet, J.L. Rouvière, N.T. Pelekanos, *Phys. Rev. B* 58 (1998) R15989.
- [33] J. Simon, N.T. Pelekanos, C. Adelman, E. Martínez-Guerrero, R. André, B. Daudin, Le Si Dang, H. Mariette, *Phys. Rev. B* 68 (2003) 035312.
- [34] C. Adelman, S. Fanget, E. Sarigiannidou, D. Jalabert, Y. Hori, T. Shibata, M. Tanaka, J.L. Rouvière, C. Bru-Chevallier, B. Daudin, *Appl. Phys. Lett.* 82 (2003) 4154.
- [35] T. Bretagnon, P. Lefebvre, P. Valvin, R. Bardoux, T. Guillet, T. Taliercio, B. Gil, N. Grandjean, F. Semond, B. Damilano, A. Dussaigne, J. Massies, *Phys. Rev. B* 73 (2006) 113304.
- [36] A.D. Andreev, E.P. O'Reilly, *Phys. Rev. B* 62 (2000) 15851.
- [37] V. Ranjan, G. Allan, C. Priester, C. Delerue, *Phys. Rev. B* 68 (2003) 115305.
- [38] T. Bretagnon, S. Kalliakos, P. Lefebvre, P. Valvin, B. Gil, N. Grandjean, A. Dussaigne, B. Damilano, J. Massies, *Phys. Rev. B* 68 (2003) 205301.
- [39] S. Kalliakos, T. Bretagnon, P. Lefebvre, T. Taliercio, B. Gil, N. Grandjean, B. Damilano, A. Dussaigne, J. Massies, *J. Appl. Phys.* 96 (2004) 180.
- [40] S. Kako, K. Hoshino, S. Iwamoto, S. Ishida, Y. Arakawa, *Appl. Phys. Lett.* 85 (2004) 64.
- [41] D. Simeonov, A. Dussaigne, R. Butté, N. Grandjean, *Phys. Rev. B* 77 (2008) 075306.
- [42] S. Kalliakos, P. Lefebvre, T. Taliercio, *Phys. Rev. B* 67 (2003) 205307.
- [43] S. De Rinaldis, I. D'Amico, F. Rossi, *Phys. Rev. B* 69 (2004) 235316.
- [44] S. Kalliakos, X.B. Zhang, T. Taliercio, P. Lefebvre, B. Gil, N. Grandjean, B. Damilano, J. Massies, *Appl. Phys. Lett.* 80 (2002) 428.
- [45] M. Tchernycheva, L. Nevou, L. Doyennette, F.H. Julien, E. Warde, F. Guillot, E. Monroy, E. Bellet-Amalric, T. Remmele, M. Albrecht, *Phys. Rev. B* 73 (2006) 125347.
- [46] C. Gmachl, H.M. Ng, S.-N.G. Chu, A.Y. Cho, *Appl. Phys. Lett.* 77 (2000) 3722.
- [47] Kh. Moumanis, A. Helman, F. Fossard, M. Tchernycheva, A. Lusson, F.H. Julien, B. Damilano, N. Grandjean, J. Massies, *Appl. Phys. Lett.* 82 (2003) 868.
- [48] L. Doyennette, L. Nevou, M. Tchernycheva, A. Lupu, F. Guillot, E. Monroy, R. Colombelli, F.H. Julien, *Electron. Lett.* 41 (2005) 1077.
- [49] A. Vardi, N. Akopian, G. Bahir, L. Doyennette, M. Tchernycheva, L. Nevou, F.H. Julien, F. Guillot, E. Monroy, *Appl. Phys. Lett.* 88 (2006) 143101.
- [50] C. Santori, S. Götzinger, Y. Yamamoto, S. Kako, K. Hoshino, Y. Arakawa, *Appl. Phys. Lett.* 87 (2005) 051916.
- [51] S. Kako, C. Santori, K. Hoshino, S. Götzinger, Y. Yamamoto, Y. Arakawa, *Nature Mat.* 5 (2006) 887.
- [52] T. Nakaoka, S. Kako, Y. Arakawa, *Physica E* 32 (2006) 148.
- [53] T. Nakaoka, S. Kako, Y. Arakawa, *Phys. Rev. B* 73 (2006) 121305.
- [54] A.F. Jarjour, R.A. Oliver, A. Tahraoui, M.J. Kappers, C.J. Humphreys, R.A. Taylor, *Phys. Rev. Lett.* 99 (2007) 197403.
- [55] J. Renard, R. Songmuang, C. Bougerol, B. Daudin, B. Gayral, *Nano Lett.* 8 (2008) 2092.
- [56] R. Bardoux, T. Guillet, P. Lefebvre, T. Taliercio, T. Bretagnon, S. Rousset, B. Gil, F. Semond, *Phys. Rev. B* 74 (2006) 195319.
- [57] R. Bardoux, T. Guillet, B. Gil, P. Lefebvre, T. Bretagnon, T. Taliercio, S. Rousset, F. Semond, *Phys. Rev. B* 77 (2008) 235315.
- [58] D. Gammon, E.S. Snow, B.V. Shanabrook, D.S. Katzer, D. Park, *Phys. Rev. Lett.* 76 (1996) 3005.
- [59] V.D. Kulakovskii, G. Bacher, R. Weigand, T. Kümmell, A. Forchel, E. Borovitskaya, K. Leonardi, D. Hommel, *Phys. Rev. Lett.* 82 (1999) 1780.
- [60] L. Besombes, K. Kheng, D. Martrou, *Phys. Rev. Lett.* 85 (2000) 425.
- [61] M. Bayer, G. Ortner, O. Stern, A. Kuther, A.A. Gorbunov, A. Forchel, P. Hawrylak, S. Fafard, K. Hinzer, T.L. Reinecke, S.N. Walck, J.P. Reithmaier, F. Klopff, F. Schäfer, *Phys. Rev. B* 65 (2002) 195315.
- [62] E. Poem, J. Shemesh, I. Marderfeld, D. Galushko, N. Akopian, D. Gershoni, B.D. Gerardot, A. Badolato, P.M. Petroff, *Phys. Rev. B* 76 (2007) 235304.
- [63] E. Martínez-Guerrero, C. Adelman, F. Chabuel, J. Simon, N.T. Pelekanos, G. Mula, B. Daudin, G. Feuillet, H. Mariette, *Appl. Phys. Lett.* 77 (2000) 809.
- [64] J.P. Garayt, J.M. Gérard, F. Enjalbert, L. Ferlazzo, S. Founta, E. Martínez-Guerrero, F. Rol, D. Araujo, R. Cox, B. Daudin, B. Gayral, Le Si Dang, H. Mariette, *Physica E* 26 (2005) 203.
- [65] D. Lagarde, A. Balocchi, H. Carrère, P. Renucci, T. Amand, X. Marie, S. Founta, H. Mariette, *Phys. Rev. B* 77 (2008) R041304.

- [66] P. Waltereit, O. Brandt, A. Trampert, H.T. Grahn, J. Menniger, M. Ramsteiner, M. Reiche, K.H. Ploog, *Nature* 406 (2000) 865.
- [67] S. Founta, C. Bougerol, H. Mariette, B. Daudin, P. Vennéguès, *J. Appl. Phys.* 102 (2007) 074304.
- [68] B. Amstatt, J. Renard, C. Bougerol, E. Bellet-Amalric, B. Gayral, B. Daudin, *J. Appl. Phys.* 102 (2007) 074913.
- [69] A. Cros, J.A. Budagosky, A. García-Cristóbal, N. Garro, A. Cantarero, S. Founta, H. Mariette, B. Daudin, *Phys. Status Solidi B* 243 (2006) 1499.
- [70] S. Founta, F. Rol, E. Bellet-Almaric, J. Bleuse, C. Moisson, B. Daudin, B. Gayral, H. Mariette, *Appl. Phys. Lett.* 86 (2005) 171901.
- [71] N. Garro, A. Cros, J.A. Budagosky, A. Cantarero, A. Vinattieri, M. Gurioli, S. Founta, H. Mariette, B. Daudin, *Appl. Phys. Lett.* 87 (2005) 011101.
- [72] F. Rol, S. Founta, H. Mariette, B. Daudin, Le Si Dang, J. Bleuse, D. Peyrade, J.-M. Gérard, B. Gayral, *Phys. Rev. B* 75 (2007) 125306.
- [73] L. Besombes, K. Kheng, L. Marsal, H. Mariette, *Phys. Rev. B* 63 (2001) 155307.
- [74] B. Rau, P. Waltereit, O. Brandt, M. Ramsteiner, K.H. Ploog, J. Puls, F. Henneberger, *Appl. Phys. Lett.* 77 (2000) 3343.
- [75] R. Mata, N. Garro, A. Cros, J.A. Budagosky, A. Garcia-Cristóbal, A. Vinattieri, M. Gurioli, E. Bellet-Amalric, S. Founta, B. Daudin, *Physica Status Solidi A*, in press.
- [76] J. Renard, C. Bougerol, E. Bellet-Amalric, B. Daudin, B. Gayral, B. Amstatt, *J. Appl. Phys.*, in press.
- [77] S. Christopoulos, G. Baldassarri von Högersthal, A.J. Grundy, P.G. Lagoudakis, A.V. Kavokin, J.J. Baumberg, G. Christmann, R. Butté, E. Feltin, J.-F. Carlin, N. Grandjean, *Phys. Rev. Lett.* 98 (2007) 126405.